



Published in final edited form as:

*Sci Transl Med.* 2019 January 02; 11(473): . doi:10.1126/scitranslmed.aao5253.

## Sex differences in GBM revealed by analysis of patient imaging, transcriptome, and survival data

Wei Yang<sup>1</sup>, Nicole M. Warrington<sup>2</sup>, Sara J. Taylor<sup>2</sup>, Paula Whitmire<sup>3</sup>, Eduardo Carrasco<sup>3</sup>, Kyle W. Singleton<sup>3</sup>, Ningying Wu<sup>4,10</sup>, Justin D. Lathia<sup>5</sup>, Michael E. Berens<sup>6</sup>, Albert H. Kim<sup>7,8</sup>, Jill S. Barnholtz-Sloan<sup>9</sup>, Kristin R. Swanson<sup>3,10</sup>, Jingqin Luo<sup>#4,11</sup>, and Joshua B Rubin<sup>#2,8</sup>

<sup>1</sup>Department of Genetics, Washington University School of Medicine, St Louis, MO, 63110,

<sup>2</sup>Department of Pediatrics, Washington University School of Medicine, St Louis, MO, 63110,

<sup>3</sup>Precision Neurotherapeutics Innovation Program, Mathematical NeuroOncology Lab, Mayo Clinic, Phoenix AZ, 85054

<sup>4</sup>Department of Surgery, Division of Public Health Sciences, Washington University School of Medicine, St Louis, MO, 63110,

<sup>5</sup>Department of Cellular and Molecular Medicine, Lerner Research Institute, Cleveland Clinic, Cleveland, OH, 44195,

<sup>6</sup>Cancer & Cell Biology Division, TGen, Phoenix, AZ, 85004

<sup>7</sup>Department of Neurosurgery, Washington University School of Medicine, St Louis, MO, 63110,

<sup>8</sup>Department of Neuroscience, Washington University School of Medicine, St Louis MO, 63110,

<sup>9</sup>Case Comprehensive Cancer center, Case Western Reserve University, Cleveland, OH, 44106,

<sup>10</sup>School of Mathematical and Statistical Sciences, Arizona State University, Tempe, AZ, 85281

<sup>11</sup>Siteman Cancer Center Biostatistics Core, Washington University School of Medicine, St Louis, MO, 63110,

# These authors contributed equally to this work.

### Abstract

\* Authors for correspondence. These authors contributed equally: Joshua B. Rubin Department of Pediatrics, Washington University School of Medicine, Campus Box 8208, 660 South Euclid Ave, St Louis, MO 63110, Phone: 314-286-2790, rubin\_j@wustl.edu. Jingqin Luo, Department of Surgery, Washington University School of Medicine, CB8100, 660 South Euclid Ave, St Louis, MO 63110, Phone: 314-362-3718, jingqinluo@wustl.edu.

**Author contributions:** JBR and KRS conceived of the experiments. WY, PW, JL, KRS, JBR designed the experiments, WY, SJT, NMW, EC, KWS, NW, JDL, MEB, JSB-S, KRS, JL and JBR analyzed data, AHK generated the GBM cell lines, SJT, NMW, JBR generated the histopathology data. All authors contributed to writing and editing the manuscript.

**Competing interests:** AHK served as a paid consultant for Monterris and received a Stryker Research Grant to evaluate outcomes after neurosurgical use of their dural substitute. KRS served as a scientific advisor for the James S. McDonnell Foundation. All other authors declare that they have no competing interests.

**Data and materials availability:** In accordance with Mayo Clinic IRB restrictions, all data used for imaging-based analyses in this manuscript are provided as tables in the supplement. As is typical of all protected patient data, we have a clinical research repository that can only be shared per specific IRB requirements. By reasonable request, by contacting Dr. Swanson, we may be able to create a data sharing agreement to share other data with interested institutions, following our institutional guidelines as well as those of the recipient. All other data associated with this study are present in the paper or supplementary materials.

Sex differences in the incidence and outcome of human disease are broadly recognized, but in most cases, not sufficiently understood to enable sex-specific approaches to treatment. Glioblastoma (GBM), the most common malignant brain tumor, provides a case in point. Despite well-established differences in incidence and emerging indications of differences in outcome, there are few insights that distinguish male and female GBM at the molecular level or allow specific targeting of these biological differences. Here, using a quantitative imaging-based measure of response, we found that standard therapy is more effective in female compared to male GBM patients. We then applied a computational algorithm to linked GBM transcriptome and outcome data and identified sex-specific molecular subtypes of GBM in which cell cycle and integrin signaling are the critical determinants of survival for male and female patients, respectively. The clinical utility of cell cycle and integrin signaling pathway signatures was further established through correlations between gene expression and in vitro chemotherapy sensitivity in a panel of male and female patient-derived GBM cell lines. Together these results suggest that greater precision in GBM molecular subtyping can be achieved through sex-specific analyses and that improved outcomes for all patients might be accomplished by tailoring treatment to sex differences in molecular mechanisms.

### One Sentence Summary:

Male and female glioblastomas are biologically distinct, and improving outcomes may require sex-specific approaches to treatment.

---

## Introduction

Current epidemiological data indicate that sex differences exist in the incidence of cardiovascular disease, disorders of the immune system, depression, addiction, asthma, and cancers [1–4], including glioblastoma (GBM) [5]. Although sex differences in disease incidence and severity may parallel variation in circulating sex hormone concentrations, in many cases, sex differences exist across all stages of life, indicating some independence from acute hormone action [3, 6]. Sex differences in GBM are evident in all age groups and therefore cannot be solely the consequence of activational effects of sex hormones [5, 7–11]. Enumerating the molecular bases for sex differences in GBM is likely to reveal fundamental modulators of cancer risk and outcome, as well as guide sex-specific components of precision medicine approaches to cancer treatment.

Identifying the basis for sex differences in cancer biology cannot be accomplished by analysis of merged male and female datasets. Instead, it requires comparison of results from parallel analyses of male and female data. The importance of this was recently highlighted in a study of asthma, a disease driven by both genetic and environmental factors, which occurs in twice as many boys as girls. Mersha *et al.* examined the influence of genetic variants on asthma, including an analysis of shared and sex-specific variant effects [2]. Of 47 variants that correlated with asthma risk in the sex-specific analyses, only 21 were detected in the combined analysis, suggesting that biologically important mechanisms of disease were obscured by a “net cancelling effect” that arose from opposing effects of genetic variation in sexes. A similar effect was observed in neurofibromatosis 1 (NF1)-associated low-grade gliomas. Despite equal tumor incidence in males and females, polymorphisms in *AC8* in

patients with NF1 increased the risk of low-grade glioma in female patients but reduced the risk in male patients [12]. The effect of *AC8* polymorphisms, which may be related to the mechanistic role of cAMP in NF1-associated glioma [13, 14], were unapparent without a sex-specific analysis due to the net canceling effect.

Whereas low-grade glioma incidence is nearly identical in males and females, malignant brain tumors in general occur more commonly in males, regardless of patient age or geographical location [5, 11, 15, 16]. As shown in recent reports, GBM occurs with a male to female ratio of 1.6:1 [5, 8–10]. In particular, although the understanding of molecular subtypes of GBM is still evolving [17], three of the four originally described transcriptional subtypes of GBM - Mesenchymal, Proneural, and Neural GBM - exhibit a 2:1 male to female incidence ratio, whereas Classical GBM occurs with equal incidence [15, 18]. To date, analyses of the transcriptome data from which these molecular subtypes were derived have been performed with merged male-female data and have not yielded insights into the molecular basis for sex differences in GBM incidence.

In addition to sex differences in incidence, emerging analyses suggest that patient outcomes may also differ between males and females in the pediatric [19] and adult GBM patient populations [20]. In a study analyzing more than 27,000 patients, Trifiletti *et al.* found that female sex was associated with longer survival [10], as did Ostrom *et al.* in an analysis of 5,372 GBM cases from the National Cancer Institute's Surveillance, Epidemiology and End Results (SEER) program and an additional 228 GBM cases from the Ohio Brain Tumor Study [20]. Similarly, female patients exhibited longer survival from gliosarcoma [8], and being female was associated with better outcome in a nomogram for predicting GBM patient survival [9]. Thus, the elucidation of sex-specific mechanisms in GBM has the potential to improve outcome for all patients by refining our understanding of disease causation and treatment response.

Here, we performed quantitative analyses of therapeutic responses in male and female GBM patients using a validated magnetic resonance imaging-based method for calculating tumor growth velocities. We also applied a computational algorithm to male and female GBM transcriptome data to gain insights into the relevance and biological basis of sex differences in GBM. Our studies indicate that standard treatment is more effective for females than for males with GBM and that, for the current standard of care - surgery, radiation, and temozolomide chemotherapy - survival in males is correlated with the expression of cell cycle regulators, whereas in females it is correlated with the expression of integrin signaling pathway components. These studies provide a coherent view of sex differences in GBM biology and their clinical ramifications. They support the development of diagnostics and treatments that incorporate sex differences in GBM biology.

## Results

### Standard treatment is more effective in female compared to male GBM patients

Sex differences in GBM incidence have been repeatedly reported [5, 7–11], and recent studies have suggested that being female is associated with better outcome from GBM in both adults and children [8–10, 19, 20]. The introduction of temozolomide as a component

of tri-modal care for adults with GBM has improved outcomes and highlighted factors, like O<sup>6</sup>-methylguanine DNA methyltransferase (MGMT) promoter methylation, that impact response and survival [21, 22]. Thus, we wondered whether sex differences in GBM survival are a consequence of differential treatment effects on male versus female patients. To answer this question, we used a magnetic resonance (MR) imaging data-based analysis, with which the velocity of radial tumor expansion can be determined [23–26]. Growth velocity, which correlates with outcome [27, 28], was measured approximately every two months in a cohort of 63 GBM patients (40 male and 23 female) treated with standard-of-care surgery, focal irradiation (XRT), and systemic temozolomide (TMZ) chemotherapy (fig. S1) [21, 22]. Analysis of serial MR images obtained during post-radiation maintenance TMZ treatment indicated that female patients exhibited a greater response to treatment than male patients. Although the initial tumor growth velocities were similarly distributed in male and female patients (Fig. 1A, Wilcoxon rank sum test  $p=0.3985$ ), a steady and significant decline in growth velocity during TMZ treatment was only evident for female patients (Fig. 1A, female trend test  $p=0.02569$ , male trend test  $p=0.1186$ ). To determine whether the initial TMZ velocity correlated equivalently with survival across sexes, we fit a Cox proportional hazard model with the main effect of velocity (in continuous scale) for the male and female populations separately and found that the velocity had a sex-specific impact on survival (male  $p=0.302$ , female  $p=0.0161$ ). To visualize the sex-specific effect, we performed an iterative Kaplan-Meier analysis in male and female GBMs separately to divide male and female patients into high versus low velocity groups and tested the survival difference using the Log-Rank test. For female patients, lower first TMZ velocity was associated with a significantly longer survival compared to female patients with higher velocity (Fig. 1B, median survival 3090 days vs 681 days,  $p = 0.00817$ ). In contrast, male patients exhibited no statistically significant correlation between survival and velocity (Fig. 1B, median survival 1111 days versus 533 days,  $p = 0.263$ ). To determine whether first TMZ velocities correlated with Revised Assessment in Neuro-Oncology (RANO) clinical response criteria, we compared survival, growth velocity, and RANO measures for this patient cohort. No significant correlations were detected (fig. S2). Although these data cannot distinguish between the therapeutic effects of radiation versus temozolomide, they do suggest that females with GBM may benefit more from standard treatment than males with GBM, and that this difference in response, which is detectable using tumor growth velocity measures, may contribute to their survival advantage.

To validate and further investigate the basis for this difference in response, we applied an established mathematical model of glioma proliferation and invasion [25, 26, 29]. We examined the pre-surgical MRIs (T1-gadolinium and T2 sequences) of 53 patients from the original growth velocity cohort combined with an additional independent cohort of 318 patients for a total of 371 newly diagnosed GBM patients (227 males, 144 females). We found that the distribution of estimated net infiltration rates ( $D$ , mm<sup>2</sup>/year) and net proliferation rates ( $\rho$ ), 1/year) did not differ between males and females before surgery (Fig. 1C). Next, we sought to determine which of the two components [24, 26, 30] was predictive of survival in male and female patients, separately. The sex-specific median of each component was used to unbiasedly dichotomize the patients into low and high groups. Female patients with low  $D$  ( $< 23.03$  mm<sup>2</sup>/year) had significantly longer survival (median

OS: 589 days versus 390 days,  $p = 0.0071$ ) compared to female patients with high D ( $> 23.03 \text{ mm}^2/\text{year}$ ) (Fig. 1D, **left panel**). This was in contrast to male patients for whom survival did not differ (median OS: 540 days versus 450 days,  $p = 0.614$ ) as a function of D ( $< 28.993$  versus  $>28.993 \text{ mm}^2/\text{year}$ ) (Fig. 1D, **right panel**). Rho, in contrast to D, stratified survival for both males and females. Females with low Rho ( $< 18.25$  per year) exhibited median OS of 542 days as compared to those with high Rho ( $>18.25$  per year), who exhibited median OS of 415 days (Fig. 1E, **left panel**,  $p=0.032$ ). Males with low Rho ( $< 18.25$  per year) exhibited median OS of 596 days as compared to those with high Rho ( $>18.25$  per year), who exhibited median OS of 410 days (Fig. 1E, **right panel**,  $p=0.0037$ ). In the independent analysis of the expansion cohort of 318 patients (195 males, 123 females), D and Rho had effects on survival in female patients that were similar to those described in the discovery cohort (227 male and 144 female), but neither D nor Rho stratified survival for male patients (fig. S3). Together with the established sex differences in incidence, these data suggest that the biology of male and female GBM may be distinct and that outcomes for all patients might be improved if therapies were better tailored to patient sex.

### Sex differences in GBM biology are revealed by JIVE decomposition

To gain insight into potential sex differences in GBM biology, we examined the transcriptome data available through The Cancer Genome Atlas (TCGA). Using Joint and Individual Variation Explained (JIVE) to integratively decompose the male and the female transcriptome data of the TCGA dataset into three orthogonal components, we identified the joint structure that was common to both sexes, the individual structure that was specific to each sex, and additionally, the residuals (fig. S4). The heat maps of the male joint structure across the male GBM patients and the female joint structure across the female GBM patients indicated that the joint structures extracted by JIVE closely captured the dominant molecular signatures defining the TCGA GBM subtypes (fig. S5, table S1). However, the joint component only explained ~45% of the total variance in the transcriptomes for each sex, whereas the sex-specific components, independent of the joint components, explained a large proportion of the remaining variability. Specifically, the male-specific component accounted for 38.5% of the total variability in the male transcriptome, and the female-specific component explained 33.6% of the total variability in the female transcriptome (fig. S6). The extracted male and female individual components exhibited distinct patterns compared to their counterpart joint structure, and more importantly, the male-specific component showed distinct patterns compared to the female-specific component (Fig. 2 A, B). We hypothesized that focused analyses of the extracted sex-specific components would reveal which gliomagenic mechanisms are most characteristic of male versus female GBM.

### Sex-specific clusters are identified using the TCGA sex-specific transcriptome expression

To identify sex-specific patient subgroups, we performed independent hierarchical clustering on the male and female-specific components from the JIVE decomposition. Weighted and unweighted consensus clustering was applied to the sex-specific expression to evaluate the robustness of sex-specific clustering (fig. S7A,B). To determine the optimal number of sex-specific clusters, we varied the total number of clusters from two to six for each sex (fig. S7C, D) and examined the cumulative density function (CDF) curves for the consensus

matrices (fig.S7E and F). We compared the resultant increase in area under the CDF curves (fig. S7 G, H) when the total number of clusters increased by one. The similarity among samples from each sex-specific cluster was examined to remove samples with great dissimilarity to the majority of samples in the cluster based on the Silhouette scores (right panels, fig. S7 A, B). Five male (mc1–5) and five female (fc1–5) clusters were thus identified as optimally capturing the transcriptomic subtypes within male and female TCGA data. The five male and female clusters were defined by sets of 293 genes and 283 genes (Fig. 2C), respectively, with 116 in common, but 177 unique to male clusters and 167 unique to female clusters (table S2).

Cases from multiple TCGA molecular subtypes [18] were distributed to each of the five male/female clusters (Fig. 2), indicating successful separation of the individual components from the joint structure components and increasing the likelihood that this approach could reveal sex effects on gliomagenic mechanisms. The one exception was fc3, 70% of which were Proneural subtype tumors with IDH1 mutations (7 IDH1 mutants, 3 WT). In contrast, male Proneural subtype tumors with IDH1 mutations were distributed across three of the male clusters, suggesting that IDH1 mutations may have sex-specific effects in GBM.

### Sex-specific clusters are robust to excluding IDH1 mutant cases

Current diagnostic criteria indicate that IDH1 mutant and wildtype GBM are two separate diseases [31]. Thus, we examined whether the definition of the sex-specific clusters was robust to excluding IDH1 mutant cases. We removed the IDH1 mutant and G-CIMP cases from TCGA, GSE13041, GSE16011, and Rembrandt datasets. We followed the same procedure (independent JIVE analysis, consensus clustering, and determination of optimal total number of sex-specific clusters) to identify sex-specific clusters in IDH1 wildtype cases. The majority of samples (65%–96.2%) were in agreement with their cluster assignments from the initial analysis, and mc5 was re-discovered in the IDH1 wildtype cases (Fig. 3). Because fc3 was predominantly comprised of IDH1 mutant cases, it was substantially diminished in this analysis.

### Survival differences exist among sex-specific clusters in TCGA GBM cohort

To establish the importance of the sex-specific clusters, we next determined whether the sex-specific clusters in the TCGA data were associated with differences in survival outcomes. Kaplan-Meier (KM) analyses of male/female clusters confirmed that survival differences exist among both male and female clusters (Fig. 4 A, B). Not surprisingly, fc3, in which 70% of the cases are IDH1 mutant, exhibited significantly better disease-free survival (DFS) with a median time to progression (TTP) of 1758 days compared to each of the other four female clusters (fc1 259 days,  $p=3.3e-5$ ; fc2 289 days,  $p=5e-4$ ; fc4 182 days,  $p=1.64e-4$ ; fc5 350 days,  $p=9.6e-5$ , Fig. 4A, table S3). In contrast, although IDH1 mutant cases segregated nearly equally to mc2, 3, and 5, only mc3 (median TTP 408 days) and mc5 (median TTP 262 days) were associated with prolonged DFS compared to other male clusters (mc1: 240 days,  $p=1.2e-2$  vs. mc3; mc2: 186 days,  $p=7.1e-3$  vs. mc3,  $p=2.8e-2$  vs. mc5; mc4: 158 days,  $p=7.3e-3$  vs. mc3,  $p=1.6e-2$  vs. mc5, Fig. 4B, table S3). This finding suggested that an interaction may exist between IDH1 mutation and sex-specific cluster features in males but not females in the determination of survival. To further evaluate this possibility, we

separated the IDH1 mutant patients from the sex-specific clusters (Fig. 4 C, D). Only three cases in fc3 were IDH1 wildtype and each of them was alive at 5 years (median DFS for fc3 was not calculable; fc1 256 days ( $p=1.4e-2$ ); fc2 274 days ( $p=1.7e-2$ ); fc4 182 days ( $p=3.4e-2$ ); fc5 350 days ( $p=1.2e-2$ ), Fig. 4C, table S4). Similarly, the DFS benefit of mc3 and mc5 remained intact after removal of the IDH1 mutant cases (mc3 408 days; mc5 262 days; mc1 240 days ( $p=4.2e-3$  vs. mc3)); mc2 176 days ( $p=1.5e-3$  vs. mc3), ( $p=1.5e-2$  vs. mc5)); mc4 158 days ( $p=3.1e-3$  vs. mc3), ( $p=2.1e-2$  vs. mc5)), Fig. 4D, table S5). These results suggest that the survival effects of fc3, mc3, and mc5 may be independent of IDH1 mutational status.

### Survival patterns of sex-specific clusters were independently validated

The transcriptome data of GSE13041, GSE16011, and REMBRANDT were decomposed with the JIVE principal components (PCs) from the TCGA data analysis (fig. S4), and the independent samples were assigned to the TCGA-derived sex-specific clusters based on the nearest neighbor algorithm. We then sought to validate the male and female cluster-specific survival profiles using all the independent samples. We were limited to an analysis of overall survival by data availability. The OS benefit of fc3 and mc5 was validated in these datasets (Fig. 4E, F, table S3). Using all the samples of the datasets under analyses (TCGA, GSE13041, GSE16011, REMBRANDT), median OS for fc3 was 1172 days, as compared to 416 days for fc1 ( $p=5.6e-5$ ), 378 days for fc2 ( $p=1.2e-7$ ), 423 days for fc4 ( $p=8.3e-8$ ), and 359 days for fc5 ( $p=4.2e-7$ ) (Fig. 3A, **left**, table S3). Median OS for mc5 was 620 days, as compared to 422 days for mc1 ( $p=1.4e-6$ ), 360 days for mc2 ( $p=8.8e-9$ ), 398 days for mc3 ( $p=7.9e-5$ ), and 387 days for mc4 ( $p=6.2e-6$ ) (Fig. 3A, **right**). Of the three validation datasets, only GSE16011 specified IDH1 mutational status. In this dataset, IDH1 mutant tumors were disproportionately distributed to fc3, but more broadly to multiple male clusters (tables S6, 7), similar to IDH1 distribution in the TCGA samples.

### IDH1 mutation status interacts with sex-specific clusters

IDH1 mutation confers a better prognosis in GBM [32]. The survival advantage of mc5 and fc3 was observed, irrespective of IDH1 status, and for males, IDH1 mutation distributed more equally across the clusters without consistent survival benefits (Fig. 3B, C). In IDH1 wildtype cases from the combined data (TCGA, GSE16011, REMBRANDT), mc5 was still correlated with the longest survival among the male clusters (hazard ratios ranging from 0.61 to 0.65 and  $p$  ranging from 0.0039 to 0.022, Fig. 3B, table S5), and fc3 had hazard ratios ranging from 0.26 to 0.29 compared to the other female clusters ( $p=0.0032$  to 0.0093, Fig. 3B, table S4). In IDH1 mutant cases from the combined data (TCGA, GSE16011), the sample size was too small and lacked sufficient power to render statistical significance on survival comparisons between mc5 and fc3 versus all the other male (mc1–4) and female (fc1,2,4,5) clusters, respectively, but the estimated hazard ratios for mc5 compared to the other male clusters and fc3 compared to the other female clusters were always below 1 (for mc5, hazard ratio=0.15–0.54,  $p=0.017$  vs. mc1,  $p=6.3e-5$  vs. mc4,  $p=0.12$  vs. mc2 and  $p=0.16$  vs. mc3; for fc3, hazard ratio=0.19 to 0.91,  $p=0.013$  vs. fc2) (tables S6 and 7). Thus, IDH1 mutation was validated as a good prognostic feature for both males and females (Fig. 3D). However, IDH1 mutation interacts with fc3 and mc5 cluster features differently (interaction  $P=0.07$ , Fig. 3E, table S8). Fc3 conferred longer survival regardless of the IDH1

mutation status. In contrast, IDH1 mutation further stratified survival differences among mc5 cases (Fig. 3E), such that IDH1 mutant mc5 GBM showed comparable or even slightly better survival than IDH1 mutant fc3 GBM (HR=0.79, 0.34~1.9, p=0.57, table S8), though statistically not significant. Together with the broader distribution of IDH1 mutation cases across all male sex-specific clusters, these findings indicate that IDH1 mutation interacts with sex in the determination of survival.

### Sex-specific clusters show differing survival patterns by TCGA molecular subtype

To gain further insights into cluster-specific effects on survival, we compared the survival differences of the male and female specific clusters when stratified by the original Verhaak subtypes [18]. We found a consistent cluster effect in which Neural, Mesenchymal, and Proneural specimens in mc5 and fc3 exhibited better survival than tumors of these same Verhaak subtypes that had clustered to mc1–4 or fc1, 2, 4, or 5 (fig. S8). Neither male nor female cluster effects were evident for the Classical subtype tumors, the only subtype for which there is no sex difference in incidence [15]. These data suggest that for those molecular subtypes of GBM in which sex impacts tumor incidence, sex also impacts patient survival. In addition, these findings indicate that sex can modulate the impact of specific gliomagenic mechanisms on survival, but that not all mechanisms, such as those underlying Classical subtype tumors, will be sensitive to the effects of sex.

### Pathway Analysis indicates that survival in males and females with GBM may be dependent upon different mechanisms.

The unequal effects of sex on survival for tumors of different molecular subtypes suggests that the effects of sex are not mediated solely by factors like sex hormones, whose actions would distribute equivalently across patients of a given sex regardless of their molecular subtype. Instead, these findings indicate that either tumor cell-intrinsic sex differences or an interaction between tumor-intrinsic and microenvironmental sex differences determine responsiveness to treatment and patient survival. To gain insight into possible mechanisms underlying sex-specific survival benefits, we compared the survival and transcriptome expression of fc3 and mc5.

Median survival for fc3 was 1172 days compared to 620 days for mc5 (Fig. 5A). To test whether similar or distinct mechanisms accounted for these sex differences in survival, we asked what distinguished fc3 and mc5 from the other female and male clusters, respectively. One hundred ninety-seven transcripts distinguished mc5 from the other male clusters, and 123 transcripts distinguished fc3 from the other female clusters (table S2). Using the Genomatrix Suite for pathway analysis, we found that 13 transcripts belonging to calcium/calmodulin signaling, synaptic, and other neuronal function pathways were shared between mc5 and fc3 (Fig. 5B). Examination of the female-specific transcripts revealed the Integrin signaling pathway as the most significant pathway (adjusted  $p < 0.001$ ) that distinguished fc3 from other female clusters (Fig. 5C, table S9), with nine transcripts in the pathway (labeled fc3.9). Six of the nine transcripts from this pathway (*PLAT*[33], *CHL1* [34, 35], *FERMT1* [36], *PCDH8* [37], *IGFBP2* [38, 39], *POSTM*[40]) have known roles in glioma, and three (*PLAT*, *IGFBP2*, and *POSTN*) can distinguish Proneural from Classical high-grade glioma gene signatures [41]. Six of the nine genes (*AK5*, *AMIGO2*, *PLAT*, *CHL1*, *PCDH8*,



*IGFBP2*) were downregulated in fc3 compared to other female clusters, suggesting that better survival in fc3 patients is favored by tumors with reduced integrin signaling (fig. S9).

Better outcome in mc5 was significantly (adjusted  $p < 0.001$ ) associated with Cell Cycle Regulation pathways (Fig. 5D). Seventeen transcripts (labeled mc5.17) were components of this pathway, and they included known critical regulators of mitosis such as *CDC20* (37, 38), *CKS2* (39), *PRC1* (40), *NUSAP1* (41), *PBK* (42), Cyclin B1 and B2 (43), and *KIF20A* (44). Fifteen of the 17 transcripts were significantly downregulated in mc5 compared to the other male clusters ( $p < 0.0061$  for differences in the original expression data,  $p = 1.7e-06$  for difference in male-specific expression data) and approached the expression observed in fc3 (Fig. 6A, B, fig. S10 A, A', B, B'). *NEFH* and *NEFM* were the exceptions, with each exhibiting greater expression in mc5 compared to each of the other male clusters. This suggests that treatment response and survival in males is determined by lower activity in factors that promote cell cycle progression.

Each of the 9 genes that distinguished fc3 (fc3.9) and the 17 genes that distinguished mc5 (mc5.17) from other female and male clusters were similarly expressed in male and female GBM patients overall (Fig. 6A, figs. S9, fig S10 A, A'). Thus, we wondered whether these genes might exert sex-specific effects on survival. For each transcript, we separated all male and female cases into low and high expression groups based on the amount of expression that distinguished mc5 or fc3 from the other male or female clusters. We then determined the effect on overall survival for each transcript in each sex separately. Finally, we compared the effect of the whole gene set on overall survival between males and females in the combined dataset. None of the distinguishing genes of fc3 exhibited a differential effect on survival in males compared to females (fig. S9). In contrast, although each of the downregulated cell cycle pathway genes in mc5 affected overall survival in both males and females, they exhibited a greater effect, as evidenced by smaller hazard ratios, in males compared to females (Fig. 6C, fig. S10 C, C'). Comparing the survival effects of the gene set in males and females, the hazard ratios of the 17 genes were significantly higher in males than their female counterparts (Wilcoxon signed rank test  $p=4.6e-05$ ), indicating that the gene set as a whole exerted a greater effect in males than in females, despite almost overlapping expression density of each gene in males and females (Fig. 6A, figs. S9 and S10).

### **Expression of sex-specific cluster-defining genes correlates with chemotherapy sensitivity**

Sex differences in GBM survival could result from many different cellular, tissue, or organismal factors. To further evaluate the potential prognostic value of the mc5.17 and fc3.9 gene signatures, we performed dose response analyses for temozolomide (TMZ), etoposide, lomustine (CCNU), and vincristine (VCR) in five male and four female primary GBM cell lines (fig. S11) to determine how the expression of mc5.17 and fc3.9 specific genes correlated with  $IC_{50}$  values.

Only one cell line (male B66) demonstrated appreciable MGMT expression as measured by western blot analysis (fig. S12). The temozolomide  $IC_{50}$  of this line was less than that of two other male cell lines with no MGMT expression (figs. S11 and S12), indicating that MGMT expression was not a dominant determinant of temozolomide resistance in these assays. Absolute  $IC_{50}$  values were calculated from each dose-response curve and correlated

with gene expression as determined by the Illumina HumanHT-12 v4 expression microarray for each cell line. Overall, male cell lines did not exhibit significantly higher absolute  $IC_{50}$  values than female cell lines (Fig. 7A). To determine whether the expression of mc5.17 and fc3.9 genes stratified responses for male and female cell lines, respectively, we calculated Spearman rank correlation coefficients between  $IC_{50}$  values and gene expression. Spearman rank correlation coefficients comparing the expression of the 17 genes in mc5.17 and  $IC_{50}$ s were, on average, positive for male cell lines, indicating that low expression of mc5.17 genes correlated with low  $IC_{50}$  values (high treatment efficacy) for each of the four agents, temozolomide, etoposide, lomustine, and vincristine (Fig. 7B). In contrast, in female cell lines, low expression of the mc5.17 genes predicted high  $IC_{50}$  values (low treatment efficacy). As a negative control, the distribution of the averaged correlation coefficient of 1000 random gene sets of the same size as mc5.17 with 17 randomly selected genes centered around 0, indicating no correlation, as expected. When the relationship between each fc3.9 gene and  $IC_{50}$  values for these drugs in male or female cell lines was analyzed, treatment efficacy in female but not male cell lines was predicted by fc3.9 genes. Again, 1000 random gene sets of the same size (9 randomly selected genes) were not correlated with  $IC_{50}$  for any drug (Fig. 7C).

These results indicated that sex-specific expression of these genes is predictive of survival in GBM patients and the *in vitro* efficacy of common chemotherapies. Together, these findings suggested that survival in GBM patients may be related to cell-intrinsic sex differences in mechanisms that broadly affect treatment response. To further evaluate the possibility of cell intrinsic sex-specific determinants of treatment response, we generated flank xenografts using a well-described male murine GBM model with complete loss of neurofibromin and p53 function, and activation of the EGF receptor [15, 42]. One million male GBM cells were implanted into male (n=14) or female (n=14) nude mice. We focused on male cells alone because we have previously characterized their more consistent *in vivo* tumor-forming potential as compared to their female counterparts. After establishing steady tumor growth, we treated tumor-bearing mice with temozolomide (21 mg/kg/day x 5 doses), etoposide (20 mg/kg/every other day x 3 doses), or vehicle (DMSO). We chose these two drugs as representative of agents with higher and lower  $IC_{50}$  values when tested in male GBM cells, respectively. We evaluated acute treatment responses by measuring the drugs' effects on proliferation using quantification of the percentage of nuclei that were positive for the mitotic marker phospho-histone H3 (pHH3). Consistent with our earlier results, we found that male cells formed tumors in recipient mice regardless of their sex. However, proliferation was significantly greater ( $p=0.0092$ ) in tumors growing in male compared to female mice (Fig. 7D). We further found that consistent with their *in vitro*  $IC_{50}$  values, etoposide, but not temozolomide, significantly ( $p=0.0082$ ) reduced tumor cell proliferation. We did not detect an interaction between recipient mouse sex and drug effects ( $p=0.5092$ ), indicating that in this model, even though the sex of the microenvironment can influence tumor growth rates, cell-intrinsic effects determine chemotherapy response (table S10).

## Discussion

Sex differences are increasingly recognized as important determinants of human health and disease. Although sex differences in incidence, disease phenotype, and outcome are well

described and broadly recognized, the molecular bases for sex differences beyond acute hormone actions are poorly understood. Among the obstacles to improved understanding of sex differences is the inconsistent application of methodologies into lab-based and clinical research design that can adequately detect and quantify sex differences. As an example, current epidemiological data indicate that in the United States, the male to female incidence ratio for GBM is 1.6:1 [5]. Even though substantial sex differences in the incidence of glioblastoma and other brain cancers have been recognized for decades, large-scale analyses continue to most commonly merge data from both sexes, obscuring discovery of valuable information contained in the sex differences.

Recent exceptions illustrate the value of using sex differences to highlight important elements of cancer biology and clinical response. We found that sex-specific, cell-intrinsic responses to loss of p53 function render male astrocytes more vulnerable to malignant transformation compared to female astrocytes [15]. These findings may well relate to the sex differences in glioma incidence and are consistent with other data describing sexual dimorphism in the p53 pathway, including radiographic sex differences in men and women with glioblastoma as a function of their p53 mutational status [43]. Understanding the molecular basis for sexual dimorphism in the p53 pathway and what it means with regard to cancer biology and clinical oncology remains an important area of research.

Most importantly, these studies emphasize that analyses without consideration of sex can obscure critical elements of biology and in aggregate, highlight the importance of parallel but separate analyses of male and female cells, male and female animals, and male and female patients. Here, we applied the JIVE algorithm to decompose male and female GBM transcriptome datasets of TCGA into joint and sex-specific components. We found that male and female GBM patients cluster into five distinct male and female subtypes that are distinguished by gene expression and survival. These clusters, which were identified using the TCGA transcriptome dataset, were subsequently validated in three independent datasets. Although GBM has recently been identified as a “low sex-effect” cancer at the transcriptome level [44], our analyses indicate that even genes with similar expression in males and females can impart substantial sex-specific effects on survival and yield mechanistically important information. Together with the sex-specific effects of p53 loss [15] and *Arlml* variants [45], these data suggest that the cellular and organismal sex context of gene expression impacts the consequences of oncogenic events. A similar mechanism was invoked to explain the sex-specific effects of AC8 polymorphisms, which increased the risk of low grade glioma in females, but decreased the risk in males with NF1 [12].

Most compelling in this regard are the molecular features of the longer surviving subtypes of male and female patients. IDH1 mutation is a molecular marker of a distinct form of GBM that is associated with better outcome [46, 47]. Here, we demonstrate that IDH1 mutation exhibits sex-specific survival benefit. In the combined dataset, almost all IDH1-mutant female tumors were assigned to fc3. This was the only female cluster with distinctly better outcome. In contrast, IDH1 mutations were distributed across all male clusters. Moreover, although the numbers were small, fc3 conferred a survival advantage regardless of IDH1 mutational status, whereas IDH1 mutation further stratified survival in mc5 cases. Thus, the predictive value of IDH1 mutation can be better defined in a sex-specific context. This

finding is in contrast to a recent immunohistochemical analysis of IDH1 mutation in a single cohort of 105 patients [48]. In this cohort, there were a total of nine IDH1 mutant tumors, 4 in males and 5 in females. The difference in survival for male patients (n=61) with and without IDH1 mutations reached statistical significance. This was not true for the female patients (n=44), but the sample size was small and the results were not validated in an independent cohort. The sex-specific impact of IDH1 mutation on survival will require additional evaluation.

Fc3 and mc5 shared a distinguishing signature in calcium/calmodulin signaling, with a particular representation of genes essential for synaptic function. They diverged in other molecular features, with mc5 exhibiting downregulation of mitotic spindle and cell cycle regulatory genes and fc3 exhibiting a downregulation of integrin signaling pathway components. Most compelling was the sex-specific effect on survival of genes within the cell cycle regulatory pathway, despite the fact that the component transcripts were similarly expressed in male and female tumors. These observations are consistent with the hypothesis that sex effects in cancer cannot simply be defined by gene expression, but rather need to include the potential sex differences in gene effect. A similar observation regarding sex differences in MGMT promoter methylation was recently published [48].

Among the striking results of this study is the potential harmonization between the sex differences in gene expression, in vitro drug sensitivity, MRI measures of tumor dispersion and proliferation, MRI measures of treatment response, and patient survival. The gene expression analysis identified downregulation of cell cycle progression and downregulation of integrin signaling as correlated with best survival in male and female patients, respectively. Expression of the 17- and 9-gene signatures that distinguished the longest surviving male and female cohorts, respectively, also correlated, in a sex-specific manner, with in vitro drug sensitivity as measured by IC<sub>50</sub> values for a panel of primary GBM cell lines. Moreover, we found evidence that MRI-based predictors of survival may differ for males and females with GBM. These predictors are based on measures of rates of proliferation and invasion. It would be premature to over-emphasize the relationship between the concordance in these measures and patient outcomes, but such multi-scale correlations are the goal of projects like The Human Tumor Atlas. In this regard, these findings may provide an example of how sex differences in cancer can be productively incorporated into these efforts.

The current study has several limitations that should be considered. First, the MR image analysis was performed retrospectively on a cohort collected from multiple medical institutions over the course of many years. Although the inclusion criteria were designed to mitigate inter-patient variability, imaging and treatments may have varied between institutions and patients. Additionally, the MR images were segmented and validated by trained individuals, which could introduce some inter-operator variability into calculated growth velocities. Second, although all genomic data, including DNA sequence and copy number variation, mRNA expression, as well as protein expression and post-translational modification data, should be collectively analyzed for sex-specific features, such a comprehensive data source of a large enough sample size for each component has yet to be established for sex-specific modeling. TCGA, the largest repository of GBM profiling

results, contains gene expression data for over 500 cases, but more limited data of other types. Thus, we defined sex-specific clusters primarily using mRNA gene expression data. We did, however, perform independent analyses after excluding IDH1-mutant cases to better reflect current thinking regarding IDH1-mutant GBM as a distinct disease entity from IDH1-wildtype GBM. In some cases, IDH1 mutation information was not available and G-CIMP status was used when appropriate as a surrogate. This analysis indicated that the sex-specific clusters were evident before and after excluding IDH-mutant cases, suggesting that they are robust across GBM disease types. With regard to clinical outcomes, we analyzed both disease-free survival (DFS) and overall survival (OS) in the TCGA dataset. Although sex-specific effects were greatest for DFS, this parameter was not reported in all the validation datasets, and thus we were limited to OS for the merged analyses. Missing IDH1 and G-CIMP information in most of the validation samples resulted in relatively small sample sizes when IDH1 mutation status was considered for survival analysis. Third, although evaluating chemosensitivity in the panel of patient-derived cell lines yielded important data, the relatively small number of cell lines limits their interpretation. Additional studies, with more cellular isolates and in vivo treatments, particularly those that might yield insights into the mechanisms underlying sex-specific effects of chemotherapy, will be necessary before we can rationally apply these results to clinical trial design. Finally, although it is not yet possible to ascribe a specific fraction of the survival differences between male and female GBM patients to any of the sex differences we describe, the current study does suggest that greater precision in GBM patient stratification may be achieved through sex-specific molecular subtyping and that improvements in GBM outcome might be possible with sex-specific approaches to treatment, including blocking cell cycle progression in male patients and targeting integrin signaling in female patients.

## Materials and Methods

### Study Design

This study was designed to investigate sex differences in GBM incidence and outcome. We performed three kinds of analyses to achieve this goal. First, we applied a previously validated MR image analysis method to calculate tumor growth velocities, and we applied an established mathematical model to estimate tumor proliferation and invasion rates. These parameters were derived from patient image and clinical data retrospectively collected from multiple institutions and sourced through the clinical research database at Mayo Clinic (Phoenix). We also evaluated sex-specific correlations between these growth parameters and survival. Second, we derived sex-specific molecular subtypes of GBM through discovery using TCGA data [49] and validation in three additional datasets: GSE16011 [50], GSE13041 [51], and the REMBRANDT study [52, 53]. Third, we measured sex differences in the in vitro cytotoxic effects of four common chemotherapeutics in a panel of nine (five male and four female) patient-derived GBM cell isolates. In addition, we evaluated the relative contributions of cellular sex and the sex of the microenvironment to therapeutic responses of two different chemotherapeutics by parallel implantation of male murine GBM cells into equal numbers of male and female mice. All pathology analyses were performed in a blinded fashion. All animal and human studies were approved by the appropriate Animal

and Human Studies committees at The Mayo Clinic (Phoenix) and The Washington University School of Medicine.

## Supplementary Material

Refer to Web version on PubMed Central for supplementary material.

## Acknowledgements

The content is solely the responsibility of the authors and does not necessarily represent the official views of the National Institutes of Health or Government.

### Funding

This work was supported by grants from the NIH, R01 CA174737 (JBR), R01 NS060752 (KRS), R01 CA164371 (KRS), U54 CA210180 (KRS), U54 CA143970 (KRS), U54 CA193489(KRS), NIH K08 NS081105 (AHK), NIH R01 NS094670 (AHK). The Children's Discovery Institute of Washington University (JBR), Joshua's Great Things (JBR). The James S. McDonnell Foundation, the Ivy Foundation, and the Mayo Clinic (KRS). NIH U01 CA168397 (MEB), Ben & Catherine Ivy Foundation (MEB).

## References and notes

- Gabory A, et al., Placental contribution to the origins of sexual dimorphism in health and diseases: sex chromosomes and epigenetics. *Biol Sex Differ*, 2013 4(1): p. 5. [PubMed: 23514128]
- Mersha TB, et al., Genomic architecture of asthma differs by sex. *Genomics*, 2015 106(1): p. 15–22. [PubMed: 25817197]
- Ober C, Loisel DA, and Gilad Y, Sex-specific genetic architecture of human disease. *Nat Rev Genet*, 2008 9(12): p. 911–22. [PubMed: 19002143]
- Seda O, et al., Systematic, genome-wide, sex-specific linkage of cardiovascular traits in French Canadians. *Hypertension*, 2008 51(4): p. 1156–62. [PubMed: 18259002]
- Ostrom QT, et al., CBTRUS Statistical Report: Primary Brain and Other Central Nervous System Tumors Diagnosed in the United States in 2009–2013. *Neuro Oncol*, 2016 18(suppl\_5): p. v1–v75. [PubMed: 28475809]
- Sun T, et al., An integrative view on sex differences in brain tumors. *Cell Mol Life Sci*, 2015.
- Molitoris JK, et al., Multi-institutional external validation of a novel glioblastoma prognostic nomogram incorporating MGMT methylation. *J Neurooncol*, 2017.
- Frandsen J, et al., Patterns of care and outcomes in gliosarcoma: an analysis of the National Cancer Database. *J Neurosurg*, 2017: p. 1–6.
- Gittleman H, et al., An independently validated nomogram for individualized estimation of survival among patients with newly diagnosed glioblastoma: NRG Oncology RTOG 0525 and 0825. *Neuro Oncol*, 2017 19(5): p. 669–677. [PubMed: 28453749]
- Trifiletti DM, et al., Prognostic Implications of Extent of Resection in Glioblastoma: Analysis from a Large Database. *World Neurosurg*, 2017 103: p. 330–340. [PubMed: 28427986]
- Chien LN, et al., Comparative Brain and Central Nervous System Tumor Incidence and Survival between the United States and Taiwan Based on Population-Based Registry. *Front Public Health*, 2016 4: p. 151. [PubMed: 27493936]
- Warrington NM, et al., The cyclic AMP pathway is a sex-specific modifier of glioma risk in type I neurofibromatosis patients. *Cancer Res*, 2015 75(1): p. 16–21. [PubMed: 25381154]
- Warrington NM, et al., Cyclic AMP suppression is sufficient to induce gliomagenesis in a mouse model of Neurofibromatosis-1. *Cancer Research*, 2010 70(14): p. 5717–27. [PubMed: 20551058]
- Warrington NM, et al., Spatiotemporal differences in CXCL12 expression and cyclic AMP underlie the unique pattern of optic glioma growth in neurofibromatosis type 1. *Cancer Res*, 2007 67(18): p. 8588–95. [PubMed: 17875698]

15. Sun T, et al., Sexually dimorphic RB inactivation underlies mesenchymal glioblastoma prevalence in males. *J Clin Invest*, 2014 124(9): p. 4123–33. [PubMed: 25083989]
16. Sun T, Warrington NM, and Rubin JB, Why does Jack, and not Jill, break his crown? Sex disparity in brain tumors. *Biol Sex Differ*, 2012 3: p. 3. [PubMed: 22277186]
17. Patel AP, et al., Single-cell RNA-seq highlights intratumoral heterogeneity in primary glioblastoma. *Science*, 2014 344(6190): p. 1396–401. [PubMed: 24925914]
18. Verhaak RG, et al., Integrated genomic analysis identifies clinically relevant subtypes of glioblastoma characterized by abnormalities in PDGFRA, IDH1, EGFR, and NF1. *Cancer Cell*, 2010 17(1): p. 98–110. [PubMed: 20129251]
19. McCrea HJ, et al., Sex, Age, Anatomic Location, and Extent of Resection Influence Outcomes in Children With High-grade Glioma. *Neurosurgery*, 2015 77(3): p. 443–52; discussion 452–3. [PubMed: 26083157]
20. Ostrom QT, et al., Females have the survival advantage in glioblastoma. *Neuro Oncol*, 2018 20(4): p. 576–577. [PubMed: 29474647]
21. Stupp R, et al., Effects of radiotherapy with concomitant and adjuvant temozolomide versus radiotherapy alone on survival in glioblastoma in a randomised phase III study: 5-year analysis of the EORTC-NCIC trial. *The Lancet. Oncology*, 2009 10(5): p. 459–66. [PubMed: 19269895]
22. Stupp R, et al., Radiotherapy plus concomitant and adjuvant temozolomide for glioblastoma. *The New England journal of medicine*, 2005 352(10): p. 987–96. [PubMed: 15758009]
23. Mandonnet E, et al., Continuous growth of mean tumor diameter in a subset of grade II gliomas. *Ann Neurol*, 2003 53(4): p. 524–8. [PubMed: 12666121]
24. Rockne R, et al., Predicting the efficacy of radiotherapy in individual glioblastoma patients in vivo: a mathematical modeling approach. *Phys Med Biol*, 2010 55(12): p. 3271–85. [PubMed: 20484781]
25. Swanson KR, Alvord EC Jr., and Murray JD, A quantitative model for differential motility of gliomas in grey and white matter. *Cell Prolif*, 2000 33(5): p. 317–29. [PubMed: 11063134]
26. Wang CH, et al., Prognostic significance of growth kinetics in newly diagnosed glioblastomas revealed by combining serial imaging with a novel biomathematical model. *Cancer Res*, 2009 69(23): p. 9133–40. [PubMed: 19934335]
27. Neal ML, et al., Discriminating survival outcomes in patients with glioblastoma using a simulation-based, patient-specific response metric. *PLoS One*, 2013 8(1): p. e51951.
28. Neal ML, et al., Response classification based on a minimal model of glioblastoma growth is prognostic for clinical outcomes and distinguishes progression from pseudoprogression. *Cancer Res*, 2013 73(10): p. 2976–86. [PubMed: 23400596]
29. Swanson KR, et al., Quantifying the role of angiogenesis in malignant progression of gliomas: in silico modeling integrates imaging and histology. *Cancer Res*, 2011 71 (24): p. 7366–75. [PubMed: 21900399]
30. Swanson KR, et al., Method and system for characterizing tumors. 2011, Google Patents.
31. Shirahata M, et al., Novel, improved grading system(s) for IDH-mutant astrocytic gliomas. *Acta Neuropathol*, 2018 136(1): p. 153–166. [PubMed: 29687258]
32. Sanson M, et al., Isocitrate dehydrogenase 1 codon 132 mutation is an important prognostic biomarker in gliomas. *J Clin Oncol*, 2009 27(25): p. 4150–4. [PubMed: 19636000]
33. Yamashita D, et al., miR340 suppresses the stem-like cell function of glioma-initiating cells by targeting tissue plasminogen activator. *Cancer Res*, 2015 75(6): p. 1123–33. [PubMed: 25627976]
34. Cheng L, et al., L1CAM regulates DNA damage checkpoint response of glioblastoma stem cells through NBS1. *EMBO J*, 2011 30(5): p. 800–13. [PubMed: 21297581]
35. Zhao WJ and Schachner M, Neuregulin 1 enhances cell adhesion molecule 11 expression in human glioma cells and promotes their migration as a function of malignancy. *J Neuropathol Exp Neurol*, 2013 72(3): p. 244–55. [PubMed: 23399902]
36. Bauer R, et al., Inhibition of collagen XVI expression reduces glioma cell invasiveness. *Cell Physiol Biochem*, 2011 27(3–4): p. 217–26. [PubMed: 21471710]
37. Xue J, et al., miR-182–5p Induced by STAT3 Activation Promotes Glioma Tumorigenesis. *Cancer Res*, 2016 76(14): p. 4293–304. [PubMed: 27246830]

38. Chua CY, et al., IGFBP2 potentiates nuclear EGFR-STAT3 signaling. *Oncogene*, 2016 35(6): p. 738–47. [PubMed: 25893308]
39. Phillips LM, et al., Glioma progression is mediated by an addiction to aberrant IGFBP2 expression and can be blocked using anti-IGFBP2 strategies. *J Pathol*, 2016 239(3): p. 355–64. [PubMed: 27125842]
40. Zhou W, et al., Periostin secreted by glioblastoma stem cells recruits M2 tumour-associated macrophages and promotes malignant growth. *Nat Cell Biol*, 2015 17(2): p. 170–82. [PubMed: 25580734]
41. Ducray F, et al., Anaplastic oligodendrogliomas with 1p19q codeletion have a proneural gene expression profile. *Mol Cancer*, 2008 7: p. 41. [PubMed: 18492260]
42. Kfoury N, et al., Cooperative p16 and p21 action protects female astrocytes from transformation. *Acta Neuropathol Commun*, 2018 6(1): p. 12. [PubMed: 29458417]
43. Colen RR, et al., Glioblastoma: imaging genomic mapping reveals sex-specific oncogenic associations of cell death. *Radiology*, 2015 275(1): p. 215–27. [PubMed: 25490189]
44. Yuan Y, et al., Comprehensive Characterization of Molecular Differences in Cancer between Male and Female Patients. *Cancer Cell*, 2016 29(5): p. 711–22. [PubMed: 27165743]
45. Amlin-Van Schaick JC, et al., Arlm1 is a male-specific modifier of astrocytoma resistance on mouse Chr 12. *Neuro Oncol*, 2012 14(2): p. 160–74. [PubMed: 22234937]
46. Nobusawa S, et al., IDH1 mutations as molecular signature and predictive factor of secondary glioblastomas. *Clin Cancer Res*, 2009 15(19): p. 6002–7. [PubMed: 19755387]
47. Yan H, et al., IDH1 and IDH2 mutations in gliomas. *N Engl J Med*, 2009 360(8): p. 765–73. [PubMed: 19228619]
48. Schiffgens S, et al., Sex-specific clinicopathological significance of novel (Frizzled-7) and established (MGMT, IDH1) biomarkers in glioblastoma. *Oncotarget*, 2016.
49. Goldman M, et al., The UCSC Cancer Genomics Browser: update 2015. *Nucleic Acids Res*, 2015 43(Database issue): p. D812–7. [PubMed: 25392408]
50. Gravendeel LA, et al., Intrinsic gene expression profiles of gliomas are a better predictor of survival than histology. *Cancer Res*, 2009 69(23): p. 9065–72. [PubMed: 19920198]
51. Phillips HS, et al., Molecular subclasses of high-grade glioma predict prognosis, delineate a pattern of disease progression, and resemble stages in neurogenesis. *Cancer Cell*, 2006 9(3): p. 157–73. [PubMed: 16530701]
52. Gusev Y, et al., The REMBRANDT study, a large collection of genomic data from brain cancer patients. *Sci Data*, 2018 5: p. 180158.
53. Madhavan S, et al., Rembrandt: helping personalized medicine become a reality through integrative translational research. *Mol Cancer Res*, 2009 7(2): p. 157–67. [PubMed: 19208739]
54. Alexander R, A note on averaging correlations. *Bulletin of the Psychonomic Society*, 1990.



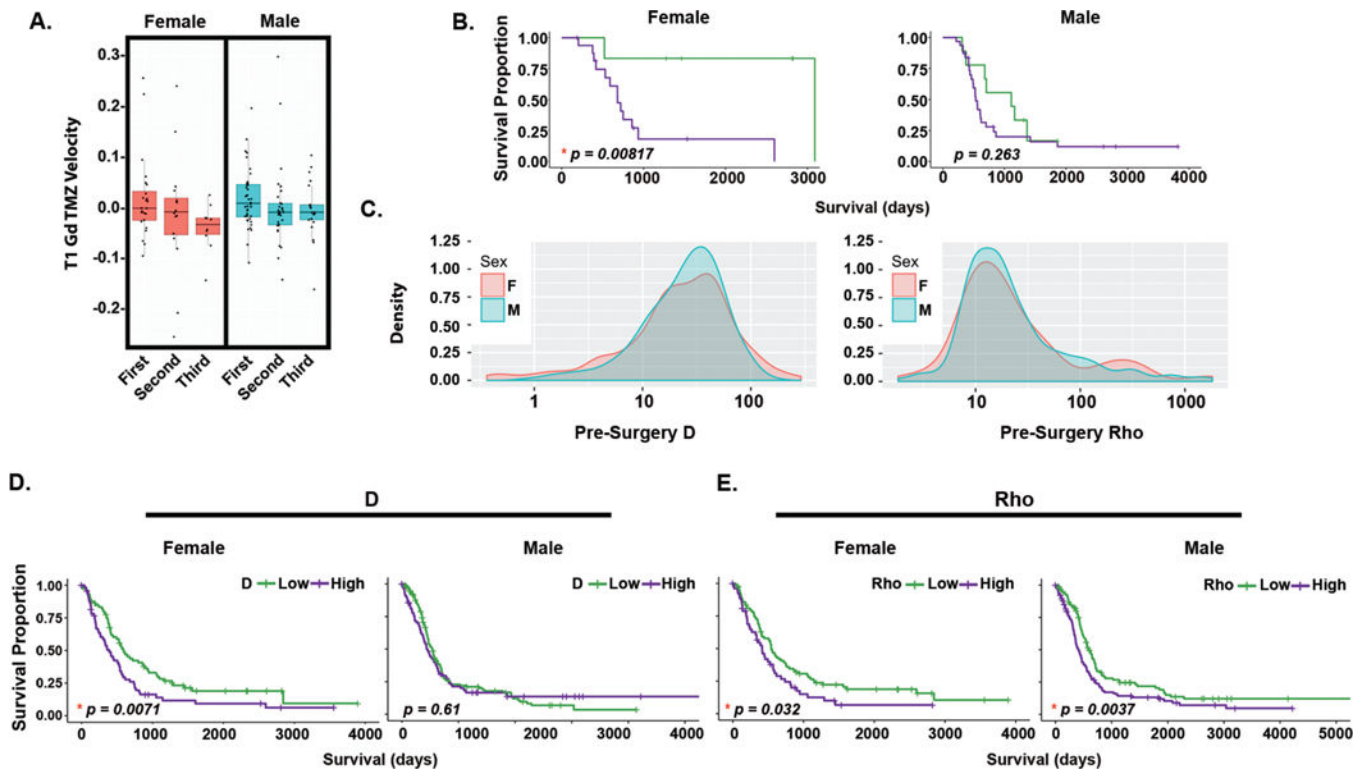


**Figure 1: Sex differences in MRI-based metrics of therapeutic responses and their correlation with survival.**

(A) Tumor growth velocities calculated from serial MR images exhibit progressive decline for female but not male patients treated with temozolomide (TMZ) in 63 GBM patients. (B) Velocity of tumor growth (low velocity = green line, high velocity = purple line) over the first temozolomide imaging interval (1–3, 28 day cycles of TMZ) stratifies female survival (log-rank,  $p=0.00817$ ), but not male survival ( $p=0.263$ ). (C) Histograms of pretreatment D and rho values in all available MRI cases (independent 53 and 318 GBM case series) for male ( $n=227$ ) and female ( $n=144$ ) patients. (D) Pretreatment D significantly stratifies survival among females ( $n=144$ , log-rank,  $p=0.0071$ ), and not among males ( $n=227$ ,  $p=0.61$ ). (E) High pretreatment rho is associated with worse survival outcomes for both females ( $n=144$ , logrank,  $p=0.032$ ) and males ( $n=227$ ,  $p=0.0037$ ).

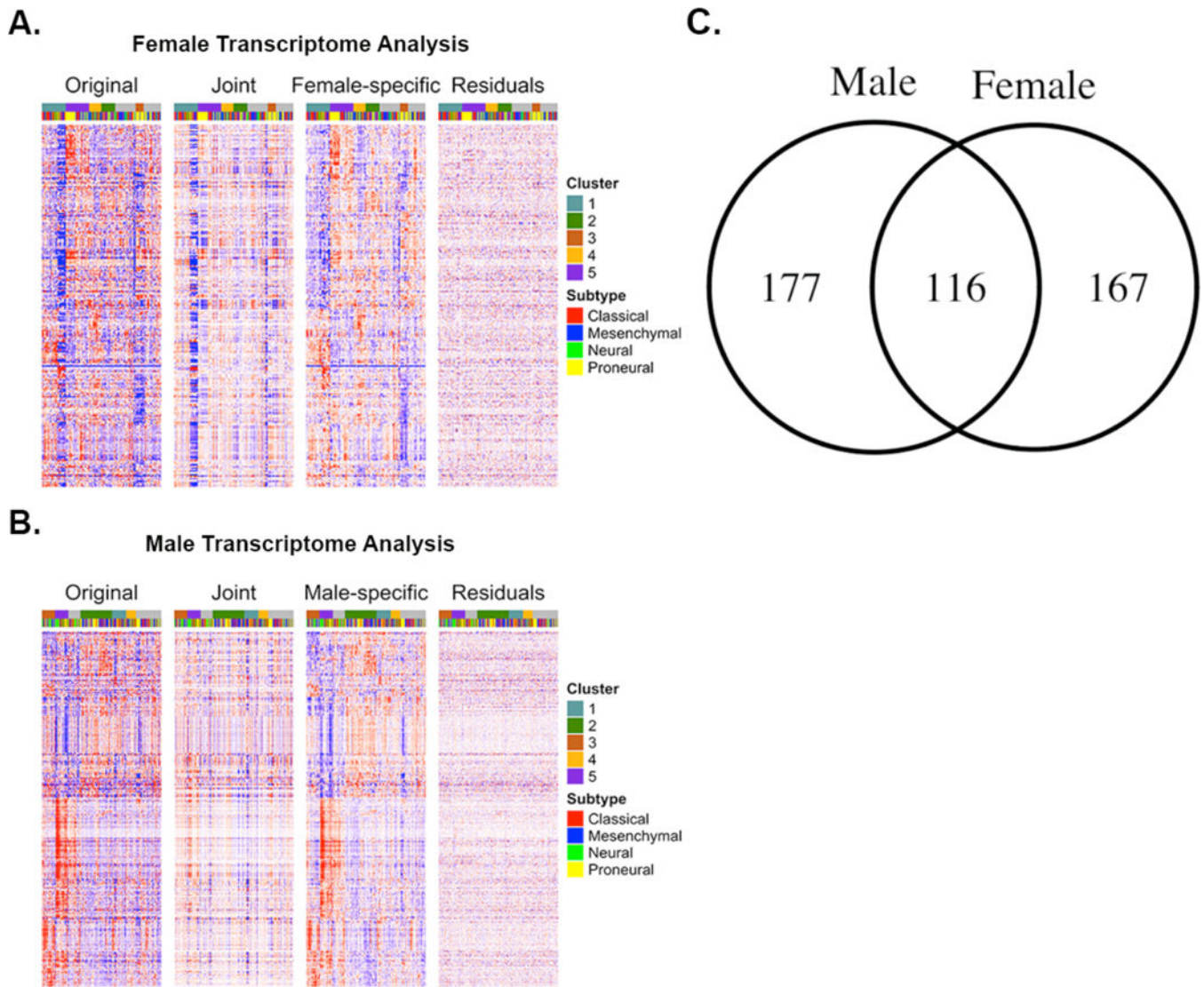


**Figure 2: Heatmaps of joint and sex-specific expression components of TCGA GBM transcriptome data revealed by JIVE.**

The heatmaps visualize each expression component. Each row represents a gene and each column a patient sample. For each patient, there are two color codes presented above the heatmap. These identify their assignment to sex-specific clusters and to TCGA molecular subtypes (gray indicates unassigned samples). Samples were ordered by sex-specific clusters. The original female (A) and male (B) expression data were decomposed into the shared expression component common to both sexes (“Joint”) and the expression component individual to each sex (“Female-specific” and “Male-specific”) and residuals as indicated. The female-relevant heatmaps (A) show 283 signature genes that define the five female-specific clusters, and the male-relevant heatmaps (B) show 293 signature genes that define the five male-specific clusters. (C) Venn diagram of male and female signature genes indicates that 116 genes are in common.

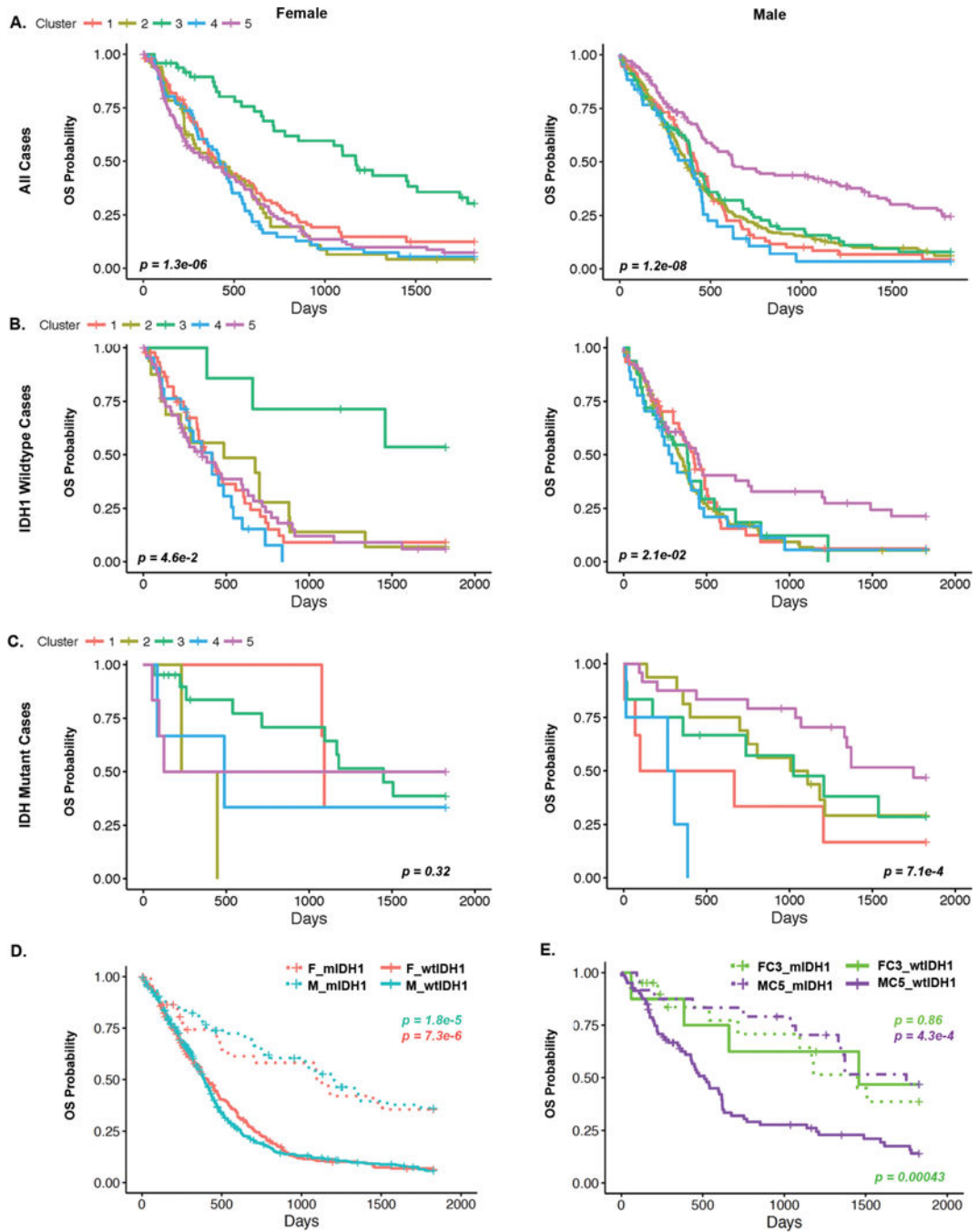


**Figure 3: Sex-specific survival effects of IDH mutation.**

(A) Overall survival benefit of fc3 and mc5 is demonstrated in the combined TCGA, GSE13041, GSE16011, and REMBRANDT datasets. See table S3 for p-values and hazard ratios. (B) Overall survival for IDH1 wildtype cases indicate that both fc3 and mc5 exert effects on survival in the absence of IDH1 mutation. (C) Overall survival in IDH1-mutant cases indicates that male-specific clusters are still associated with an effect on survival. The numbers of female IDH1-mutant cases not assigned to fc3 are n= 3, 2, 3, 6 in fc1, 2, 4 and 5 respectively, using TCGA and GSE16011 samples in combination (see table S7). (D) IDH1

mutation confers a similar survival benefit in males and females with GBM. **(E)** The survival benefit of fc3 is independent of IDH1 status. In contrast, IDH1 status exerts a significant effect on survival in mc5 cases.  $p = 4.3e-4$  for the comparison between mc5 cases with and without IDH1 mutation. Overall log rank test  $p$  value is shown comparing across all the groups presented in each panel (table S8 shows the  $p$ -values and hazard ratios for all pairwise comparisons).

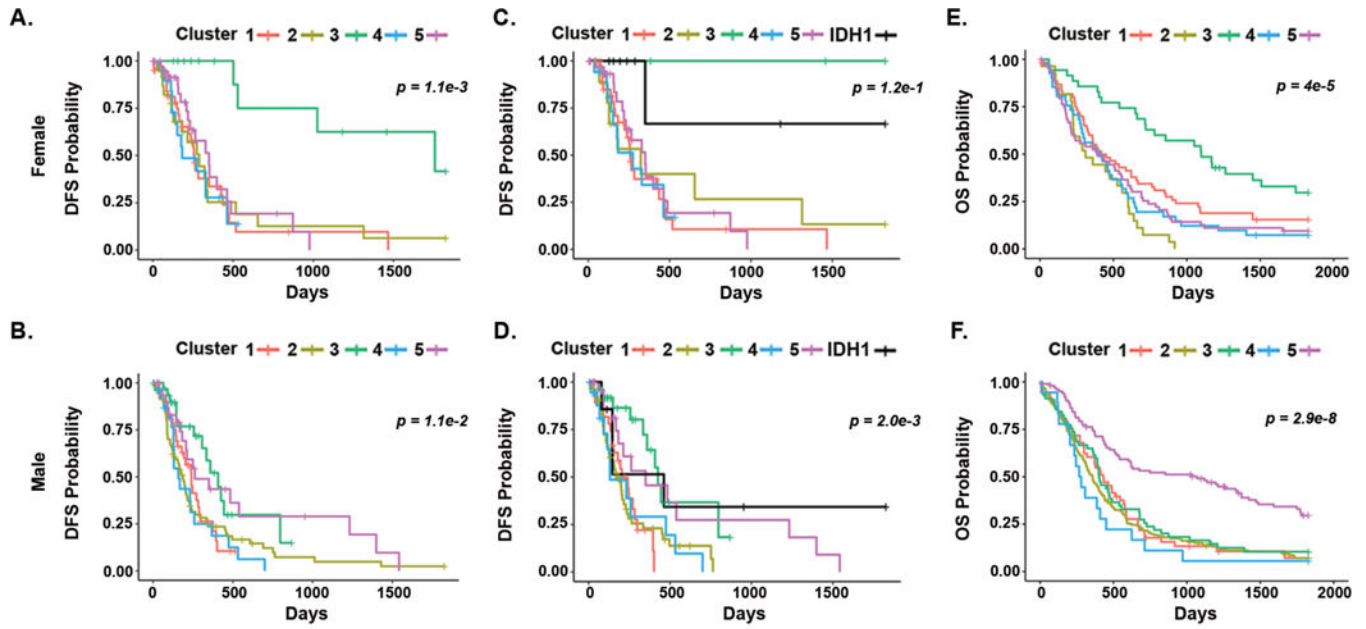


**Figure 4: Disease-free survival of sex-specific clusters in TCGA GBM dataset and overall survival of sex-specific clusters in three independent datasets combined.**

(A) Disease-free survival (DFS) in TCGA-derived female clusters (1–5). (B) DFS in TCGA-derived male clusters (1–5). (C) DFS in TCGA-derived female clusters (1–5) in which IDH1-mutant cases are plotted as an independent cluster. (D) DFS in TCGA-derived male clusters (1–5) in which IDH1-mutant cases are plotted as an independent cluster.

Independent samples combining GSE13041, GSE16011, and REMBRANDT datasets were assigned to sex-specific clusters, and the superiority of overall survival of fc3 (E) and mc5 (F) was validated in the independent samples. Overall log rank test  $p$  value is shown comparing across all the groups presented in each panel (see tables S3 and S4 for the  $p$ -values and hazard ratios for all pairwise comparisons).

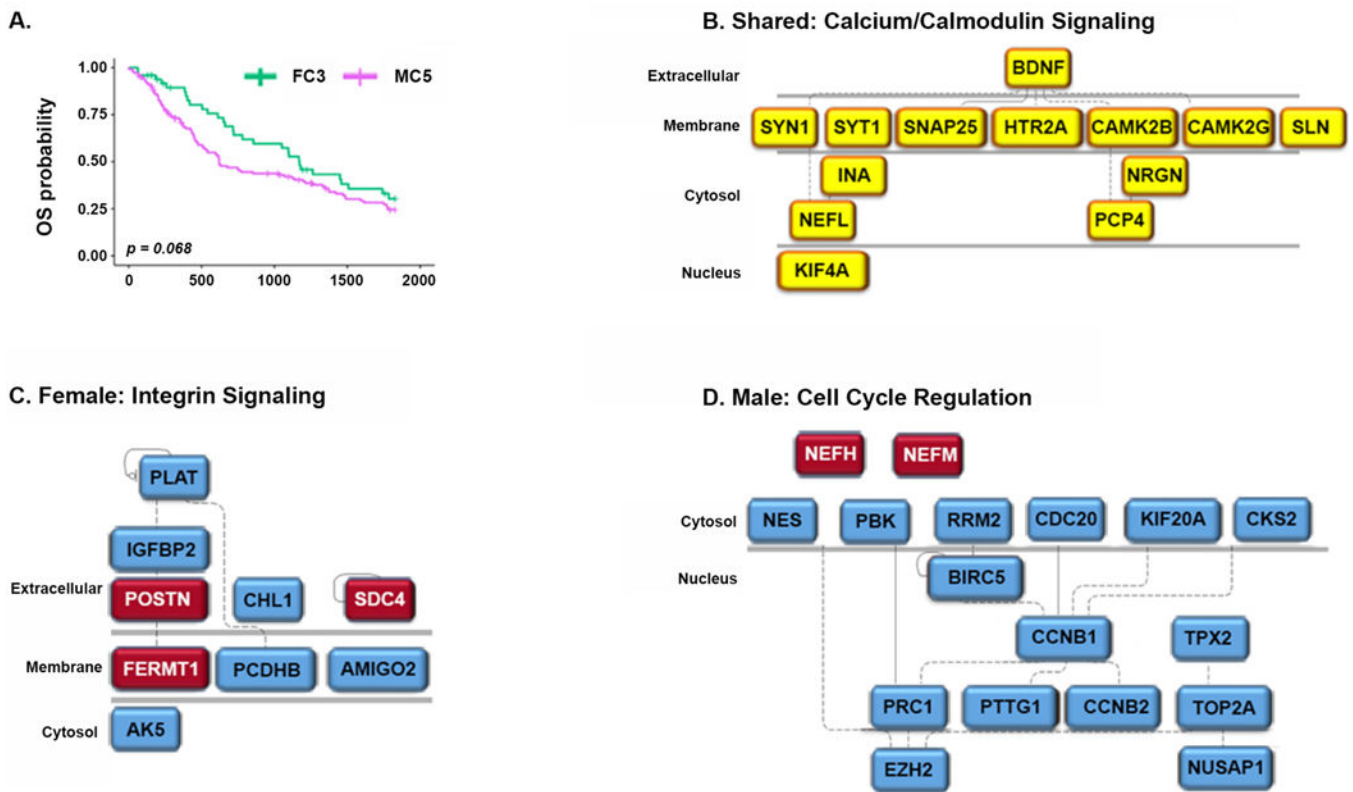


**Figure 5: Analysis of genes and pathways that mediate better survival.** (A) In the combined dataset, the survival of females assigned to female cluster 3 (median survival 1172 days) was compared to the survival of males assigned to male cluster 5 (median survival 620 days). (B-D) Genes that distinguished female cluster 3 and male cluster 5 from other female and male clusters, respectively, were compared (see table S2). Pathways in all analyses were prioritized by the combination of the numbers of genes from the pathway involved and the corrected p-value for the relevance of the pathway. (B) Calcium/calmodulin signaling was the most significantly involved shared pathway between female cluster 3 and male cluster 5 (adjusted  $p < 0.001$ ). (C) The integrin signaling pathway was the most significant female-specific pathway (adjusted p-value  $< 0.001$ , table S9). Genes that were up- and down-regulated in fc3 compared to the other female clusters are in red and blue boxes, respectively. (D) Cell cycle regulation was the most significant male-specific pathway (adjusted p-value  $< 0.001$ , table S9). Genes that were up- and down-regulated in mc5 compared to the other male clusters are in red and blue boxes, respectively. See table S2 for complete gene lists and statistics for each analysis.

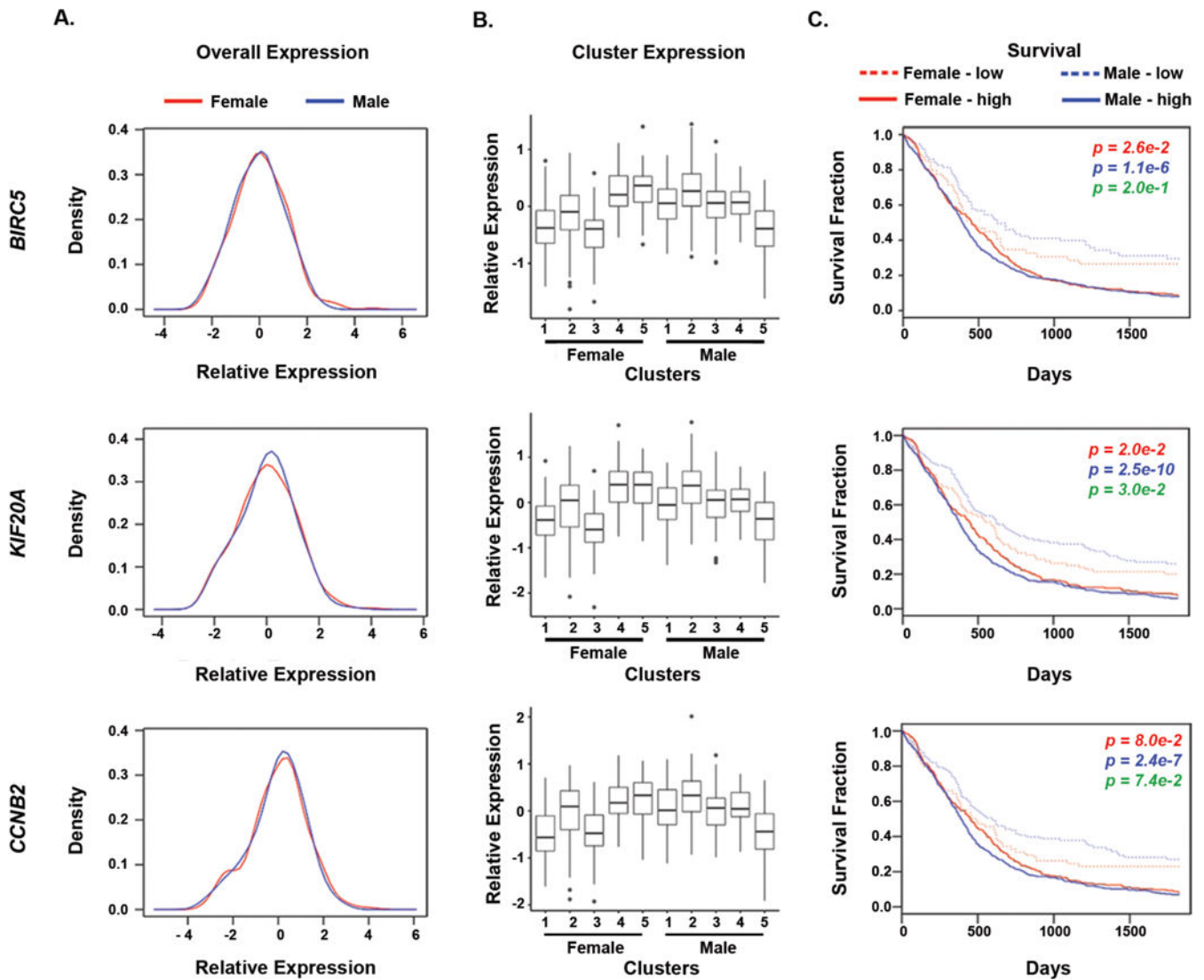


**Figure 6: Male Cluster 5-defining genes and overall survival in the merged TCGA, GSE16011, and GSE13041 dataset.**

(A) Density plots for sex-specific expression of male (in blue) and female (in red) GBM specimens of three male cluster 5 defining genes (*BIRC5*, *KIF20A*, *CCNB2*). The overlay in male and female plots indicates near identical expression in the populations. (B) Expression of each gene by sex and sex-specific clusters is presented as boxplots. (C) High and low expression groups for each gene were defined relative to the level of expression that distinguished male cluster 5 from the other male clusters (see Supplemental Material—overall sex-specific survival effects). The survival effects of differences in expression were determined for males and females. Each gene exerted a greater effect on survival in males compared to females. P-values from Cox regression model are labeled in red for comparisons between survival curves of female GBM patients with low vs. high expression of each and labeled in blue for the same survival analysis of male GBM patients. The p-value labeled in green refers to the interaction of sex and low/high expression of a gene in

Cox regression models. Parallel analyses of the female cluster 3-defining genes and the other male cluster 5-defining genes are presented in fig. S9 and fig S10, respectively.

Author Manuscript

Author Manuscript

Author Manuscript

Author Manuscript



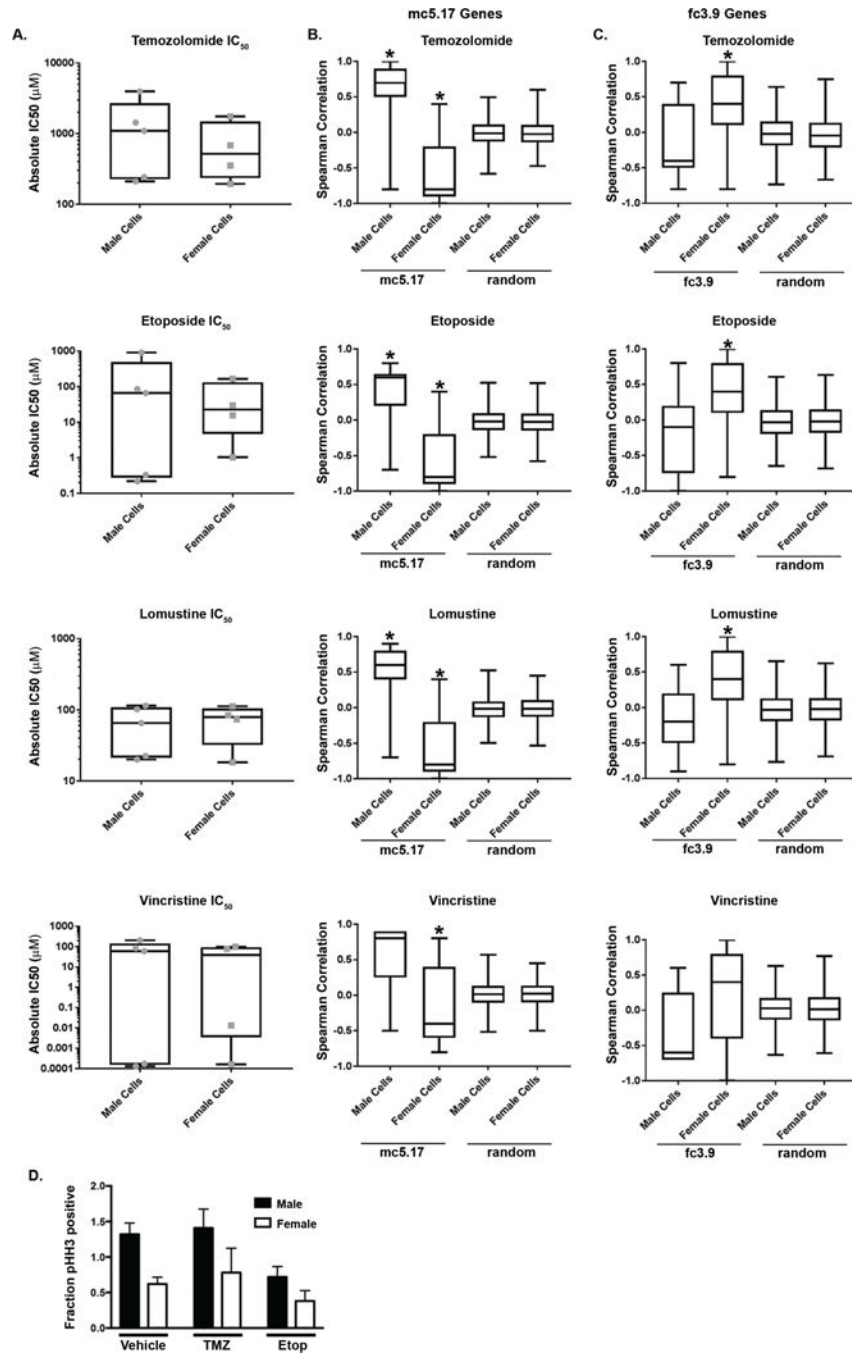


**Figure 7: Expression of cluster-defining genes and response to common chemotherapeutics in vitro.**

(A) Absolute IC<sub>50</sub> values for temozolomide, etoposide, lomustine, and vincristine for 5 male and 4 female patient-derived glioblastoma cell lines were calculated from six-point dose response curves for each cell line. Boxplots of IC<sub>50</sub> across cell lines by sex are presented (horizontal bar indicates median). Median male and female IC<sub>50</sub> values were not significantly different based on two sample t-test. Spearman correlation coefficients of IC<sub>50</sub> values for each drug with expression of mc5.17 genes (B), fc3.9 genes (C), or random gene

sets are shown in male and female cell lines. For mc5.17 and fc3.9 genes, box plots represent the distribution of the 17 or 9 cluster-defining genes, respectively, and for random gene sets, the box plots represent the distribution of the Olkin-averaged Spearman correlation coefficient [54] of 17 or 9 randomly selected genes per random gene set for 1000 random gene sets. Asterisks represent  $p < 0.01$  compared to random gene sets for each sex.

**(D)** Quantification of the percent of phospho-histone H3 (pHH3) positive nuclei in male GBM cells implanted in male (black bars) or female (white bars) nude mice. Tumor-bearing mice were treated with vehicle (DMSO), temozolomide (21 mg/kg/day x 5 days), or etoposide (20 mg/kg/every other day x 3 doses), and pHH3 positivity was determined in a blinded fashion.